How do microbes grow in nature? The role of population dynamics in microbial ecology and evolution

Justus Wilhelm Fink
Institute of Integrative Biology, Department of Environmental Systems Science, ETH Zurich, Zurich, Switzerland

Michael Manhart*
Center for Advanced Biotechnology and Medicine and Department of Biochemistry and Molecular Biology, Rutgers University, Robert Wood Johnson Medical School, Piscataway, NJ, USA
Institute of Integrative Biology, Department of Environmental Systems Science, ETH Zurich, Zurich, Switzerland and Department of Environmental Microbiology, Swiss Federal Institute of Aquatic Science and Technology (Eawag), Dübendorf, Switzerland
(Dated: February 18, 2023)

The growth of microbial populations in nature is dynamic, as the cellular physiology and environment of these populations change. Understanding the growth dynamics of these populations has wide-ranging consequences for their ecology and evolution; it may also be critical for clinical and environmental applications in which we need to promote or inhibit microbial growth. Here we review the latest efforts to measure population dynamics of microbes in natural environments. We then address the role of population dynamics, especially tradeoffs in growth traits, in mediating ecological coexistence of multiple species. Finally, we discuss how population dynamics and evolutionary processes form a feedback loop that ultimately shapes the evolved patterns of growth we observe. We identify the major gaps in our current knowledge for each of these topics and what future work will be required to close them. We conclude with a brief outlook on the future of microbial population dynamics research.

I. WHAT ARE THE POPULATION DYNAMICS OF MICROBES IN NATURAL ENVIRONMENTS?

The focus of microbiology has shifted in the last decade from the study of tractable but simplified laboratory environments to the behavior of microbes in their natural environments [1–5]. Evidence suggests that microbial populations in these environments are highly dynamic: individual taxa can grow 20-fold over the course of a week in the surface ocean [6] or fluctuate fourfold each day in the human gut microbiome [7]. However, we are still beginning to put together a quantitative picture of what these growth dynamics look like in detail [8].

There are three main scenarios for a population's growth: positive net growth (Fig. 1a), as occur for strains colonizing new environments such as the infant gut [9]; negative net growth (Fig. 1b), as has been observed for microbial taxa in anaerobic wastewater treatment [10]; or approximately zero net growth such that their abundances remain constant (Fig. 1c), which is the only scenario feasible over long times. Zero net growth can arise either because birth rates and death rates are balanced at every time point (Fig. 1d), or because birth and death occur asynchronously, such that the population spends some short periods of time undergoing net birth and other periods undergoing net death, while maintaining zero net growth over long times (Fig. 1c). Indeed, there is the possibility of different short-time scale behavior for all of these long-time scenarios (Fig. 1a,b). It is often useful to parameterize these short-time dynamics according as discrete phases of growth, each of approximately constant growth rate (Fig. 1f,g) [11]. We can then describe the high-dimensional growth dynamics as a lower-dimensional set of traits corresponding to each discrete growth phase [12, 13].

Distinguishing these scenarios is in principle straightforward given time-series data of absolute abundances. Unfortunately, measuring the absolute abundance of microbial strains in natural environments remains difficult [14] despite recent advances [9, 10, 14–16]. However, the more fundamental obstacle to measuring growth dynamics is insufficient time resolution. For example, the human gut microbiome of a single individual can be sampled at best every six hours [7] (although an average time series of resolution every two hours can be reconstructed from replicate samples at a single time point [17]), but this frequency is insufficient to capture short growth phases of 2-3 cell divisions.

An alternative strategy to the time-series approach relies instead on inferring the instantaneous birth rate of a population from a covariate property measured from a single "snapshot" in time. For example, a snapshot of the age distribution can be used to estimate birth rate in plants or animals [18, 19]. In the case of microbes, Korem et al. [20] used a mechanistic model of cell division [21] to identify the peak-to-trough ratio (PTR) of genome read coverage as a proxy for growth rate. This method performed well for *E. coli* in lab environments, and the method has since been extended to work with draft genomes [22, 23] and lower read coverage [24, 25], but neither of these implementations performed as well

* To whom correspondence should be addressed. Email: mmanhart@rutgers.edu

in additional experiments with Synecococchus [26] and a diverse marine community [25, 27]. One key limitation of PTR is that it cannot be converted into a growth rate unless the period of DNA replication is known [20, 21], which may vary across species and environments.

Since the instantaneous birth rate is a global regulator of many cellular processes, snapshot methods also have tried to correlate birth rate with other cell properties such as gene expression [28], proteome allocation [29], or other omics data [30, 31]. For these methods to measure growth rate in natural environments, they will have to be trained with measured growth rates from these habitats. Such benchmarking data sets are currently lacking, but they will have to come from time series of absolute abundance [27] or other methods that already provide calibrated growth rates. Insight into the growth rate of natural populations also comes from environmental biogeochemistry, using isotope-labeled nutrients as chemical tracers [32, 33].

A final category of methods for determining growth dynamics aims not to infer instantaneous birth rates in samples, but rather to infer properties of growth from evolved patterns in genomes. One such method uses the accumulation of mutations in a genome as a clock to determine the historical birth rate of the species, assuming that mutations occur only during cell divisions and are largely neutral [34]. Other methods in this class infer the maximum potential birth rate of a species, rather than the birth rate realized during its evolutionary history. The best genomic pattern here appears to be codon usage bias [35–37]. Figure 1e shows minimum doubling times predicted by this method, which span about two orders of magnitude from 10 minutes to 100 hours across all isolates from genome databases [37]. However, when tested in benchmark marine species, the predicted maximum birth rate falls short of matching the birth rate measured from absolute abundance data [27]. This may be because of significant differences between the environmental conditions used for the training data [35, 36] and the species' true natural environments, or because the organism simply grows at rates much slower than their maximum due to nutrient limitation. Besides codon usage bias, rRNA copy number provides another genomic pattern which can show a moderate correlation with birth rate in literature data [35, 38, 39] but mostly fails to predict the actual birth rate measured by isotope-labeled heavy water in a soil community [39].

What causes population growth to vary with time? Changes in the supply of resources are a likely factor. For example, populations may grow fast immediately after a pulse of resources, but then decelerate and eventually stop growth once the resources deplete (Fig. 1f,g,h,i). Understanding population dynamics in natural environments therefore requires understanding resource dynamics as well. One general classification we aim to determine is whether natural resource dynamics are more "chemostat-like" — where the rate of resource influx is fast compared to the rate of population growth and death, leading to an approximately constant resource abundance — or more "batch-like," where the resource influx is slow compared to population growth (e.g., resources arrive in infrequent pulses) [40]. Identifying which nutrients are limiting growth is also an important question, especially for the problem of promoting or inhibiting growth of microbial populations. For example, recent work has suggested that nitrogen is the primary limiting nutrient of microbes in mammalian guts [41], but it is also possible that multiple nutrients could simultaneously co-limit growth [42].

II. THE ROLE OF POPULATION DYNAMICS AND GROWTH TRADEOFFS IN ECOLOGICAL INTERACTIONS

The dynamic nature of population growth makes interactions between species in a community dynamic as well. This raises the possibility of distinct temporal niches for each species [43], in which one species specializes in growing at some times (e.g., while the environment is in a certain state) while the other species specializes in growing at other times. Over long periods of time, this may allow the two species to stably coexist, as formalized by concepts such as relative nonlinearity (differential responses to changing resource concentrations) and the storage effect [44]. These mechanisms are especially important to ecology because they allow for coexistence of many species on few resources [45].

The fundamental ingredient of coexistence through these temporal niches is a tradeoff in growth traits for the two species' population dynamics. Growth tradeoffs may be considered over different samples of genotypic and environmental variation (Box 1 and Fig. 2); within-population genotypic tradeoffs are required for coexistence. What would cause these tradeoffs? Besides evolution, as we will discuss in the next section, the most commonly-considered mechanism is an underlying constraint. For example, if cells have only finite resources to invest in metabolism for two different nutrients, different genotypes will have different investment strategies, creating a tradeoff between growth on those different nutrients. Two of the best-studied constraints hypothesized to affect microbial growth are the rate-yield tradeoff for metabolic pathways [48] and the rate-affinity tradeoff for nutrient uptake [49].

So what tradeoffs in microbial growth are actually realized? Existing data shows that tradeoffs across genotypes occur sometimes, but are not widespread among closely-related microbial species. Motivated by the rate-affinity tradeoff in nutrient uptake, a tradeoff in population growth rates at high and low concentrations of resources has been reported in a few systems [50], while other studies have actually found synergies across genotypes [51, 52] or no correlation at all [53]. Metabolic rate-yield tradeoffs and the concept of r/K selection have motivated testing tradeoffs in population growth

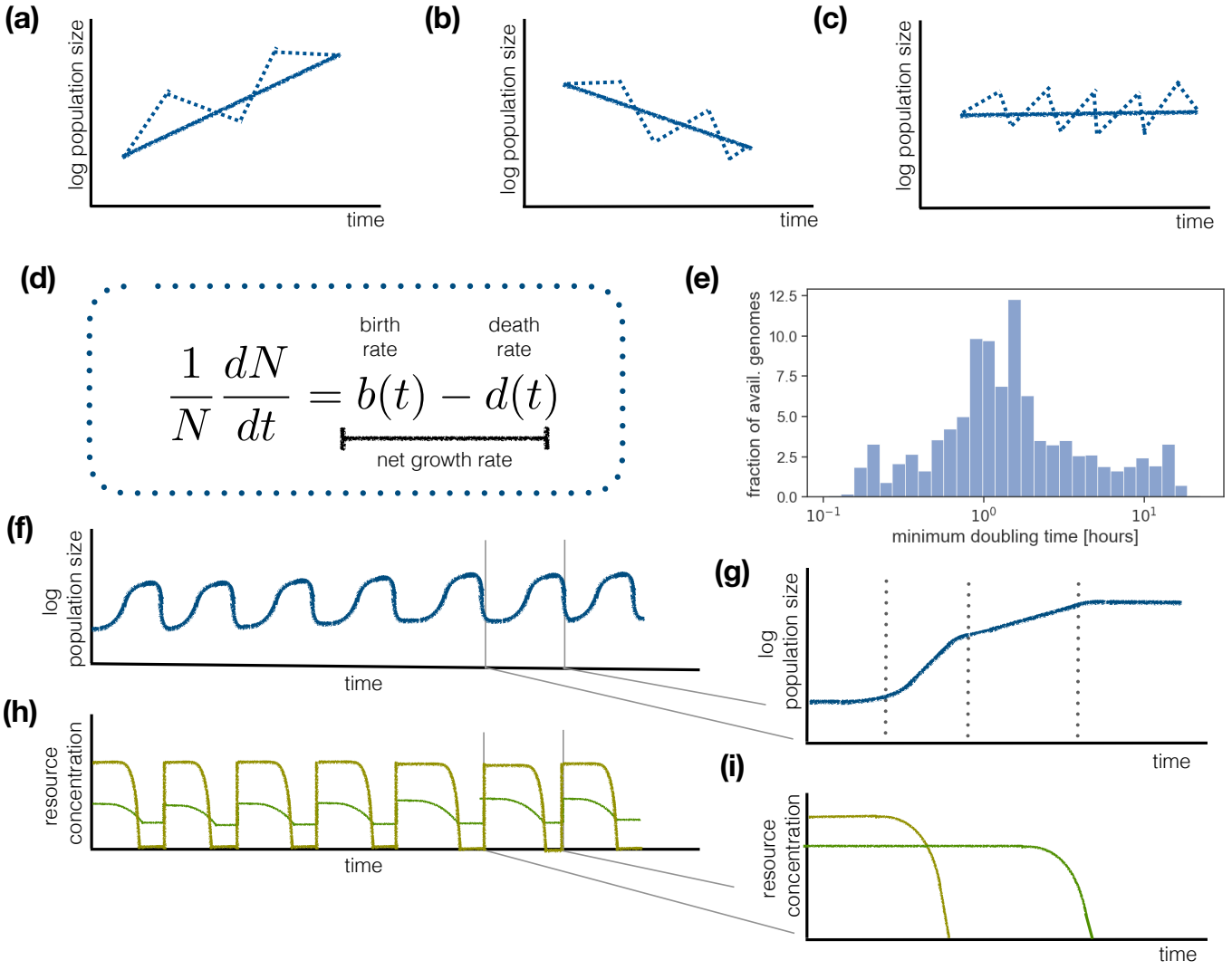

FIG. 1. **Fundamental aspects of microbial population dynamics.** (a) Schematic abundance trajectory (thick line) for a microbial population with positive net growth rate, given by the slope of the log abundance over time ($d \log N/dt$). An alternative trajectory with short-term variation in net growth rate but same total change in abundance is plotted on top (dotted line). (b) Similar to panel (a), but for a population with negative net growth rate. (c) Similar to panel (a), but for a population with zero net growth rate. (d) Decomposition of the net growth rate $d \log N/dt$ of a microbial population into birth rate $b(t)$ and death rate $d(t)$. (e) Distribution of minimum doubling times for ca. 200,000 prokaryotic genome sequences from the EGGO Database [37], as predicted from the codon usage bias of each genome. (f) Schematic time series of abundance for a microbial population with zero net growth rate on longer timescales, but with short-term cycles of growth and death. (g) Excerpt of the time series in panel (f), zoomed into a single growth cycle. Dotted lines mark separate the discrete phases of growth. (h) Schematic time series of concentrations for two abiotic resources (dark green and yellow green) that drive microbial growth in panel (f). (i) Excerpt of the time series in panel (g), zoomed into a single growth cycle.

rates and yields, with some experiments indeed detecting tradeoffs [54–57] while others finding no correlation, positive correlations, or more complex relationships between growth rate and yield [58–64]. Measurements of lag times and doubling times have also found mixed results [46, 52, 62, 65–68] (e.g., Fig. 2f). A major problem with this topic is that tradeoffs do not necessarily translate across biological scales: a rate-yield tradeoff for a single pathway may not correspond to a tradeoff for a whole cell or population. Indeed, many studies that claim these tradeoffs do not actually measure population growth, but rather a metabolic or intracellular process such as uptake [69–72].

The existence of tradeoffs alone, though, is insufficient to support coexistence of multiple genotypes; the tradeoffs must exist in the right context of population dynamics [45, 73]. For example, Bloxham et al. [74] recently found that a tradeoff in growth rates and diauxic lag times was consistent with the coexistence of two species in batch cultures. Future work on this topic will require

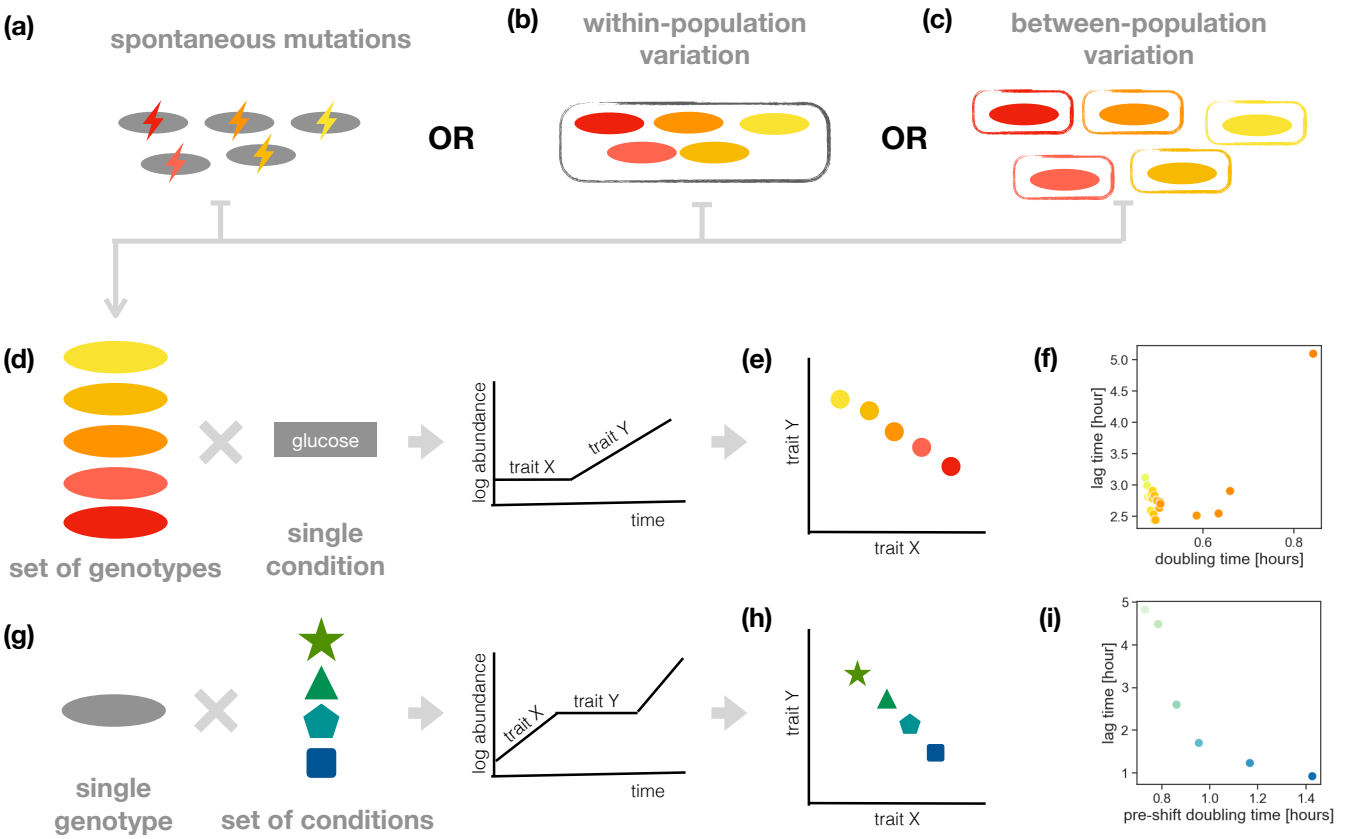

FIG. 2. **Types of tradeoffs in microbial population growth.** (a) An example set of cells (grey) that vary by spontaneous mutations to their genome (different colors). (b) An example set of cells with different genotypes (colors) that all co-occur in the same population (grey box). (c) An example set of cells that vary by genotype (colored oval and box) and occur in independent populations. (d) Schematic procedure for measuring a tradeoff across genotypes (colored ovals) in a fixed environmental condition (grey box). For each genotype, the two growth traits X and Y are identified from the strain's growth curve (black line). (e) Schematic of data showing a tradeoff across genotypes between two traits X and Y. (f) Measured doubling time (x-axis) and lag time (y-axis) for a set of *E. coli* genotypes that differ by single mutations in their adenylate kinase protein [46]. (g) Schematic procedure for measuring a tradeoff across environments (colored shapes) for a single genotype (grey oval). For each environmental conditions, two traits X (here: growth rate in first phase) and Y (here: lag time) are estimated from the growth curve (black line). (h) Schematic of data showing a tradeoff across environments between the two traits X and Y. (i) Measured doubling time before nutrient shift to acetate (x-axis) and lag time after shift to acetate (y-axis) for *E. coli* under five different pre-shift carbon sources (colors) [47].

high-throughput measurements of growth traits (rather than uptake or metabolic traits) across large strain or species libraries. In particular, this would be valuable for collections of strains or species that are already known to coexist in the same community, so we can test how much of this coexistence can be explained by any growth tradeoffs.

III. WHAT IS THE FEEDBACK BETWEEN MICROBIAL POPULATION DYNAMICS AND EVOLUTION?

Over long time scales, the existence of growth tradeoffs ultimately depends on the relationship between population dynamics and evolutionary processes. Population dynamics shape key aspects of evolution (Fig. 3a): for example, the population size determines the supply rate of new mutations and other sources of genetic variation (e.g., horizontal gene transfer), as well as the strength of demographic fluctuations (genetic drift) [75]. Population dynamics also determine the total "budget" and allocation of selection pressure across traits (Fig. 3b–e). This is because selection on mutations is proportional to the number of generations over which those mutations compete [53, 73, 76], as dictated by the population dynamics. For example, population dynamics with long lag times while transitioning into growth will have greater selection on mutations affecting lag traits (Fig. 3b–e) [73]. Different patterns of resource supply and mortality also play a major role. For example, Letten and Ludington [40] recently demonstrated in a model that population dynamics with constant resource supply and mortality (chemostat-like conditions) select for different compo-

Box 1: Types of tradeoffs in microbial growth traits. A tradeoff between two traits X and Y (e.g., lag time and doubling time) is a negative correlation in the values of those traits across some set of samples. Often the two traits are chosen such that they are both under positive selection, in which case the tradeoff has ecological and evolutionary consequences, but that is not always the case. There are two major classes of tradeoffs in population growth traits, which differ in the variation across samples they represent:

1. **Genotypic tradeoffs:** These tradeoffs describe negative correlations of traits across a set of different genotypes. One can choose the set of genotypes in various ways, but there are three most common types of genetic variation: spontaneous mutations on a specific background strain (Fig. 2a), standing variation within a population (Fig. 2b), or variation across independent populations (Fig. 2c). In any of these cases, we test existence of a tradeoff between two growth traits (e.g., lag time and minimum doubling time of a growth curve, Fig. 2d) by measuring the traits in a single environmental condition for all genotypes in the set. A genotypic tradeoff exists if there is a negative correlation between those traits across genotypes (Fig. 2e). Such tradeoffs appear to be rare for closely-related sets of genotypes. For example, Fig. 2f shows lag times and doubling times across a set of *E. coli* strains with point mutations in the adenylate kinase protein [46]; while some subsets of these mutations exhibit tradeoffs, the whole set does not at a statistical level.
2. **Environmental tradeoffs:** These tradeoffs correspond to negative correlations of traits for a single genotype across multiple environments (Fig. 2g,h). Note that this requires defining traits X and Y in a way that matches across the environmental variation. For example, Basan et al. [47] found for a single *E. coli* strain an environmental tradeoff between the doubling times in different carbon sources as well as the lag time after shifting to a different carbon source (Fig. 2i).

sitions of strains than population dynamics with pulsed resource supplies and mortality (batch-like conditions).

However, population dynamics not only shape, but are also shaped by, evolution (Fig. 3a), as mutations affecting growth traits fix. What patterns of population dynamics should we expect to evolve? Evolution occurs in two steps. First, genetic variation in growth traits is supplied to the population (Fig. 3f), usually through spontaneous mutations, horizontal gene transfer, or migration, but there can also be cryptic genetic variation that is revealed after a change in environment. Biases in the supply of growth trait variation can have a major impact on the evolved trait patterns. For example, growth phases may evolve to be short compared to lag phases if there are more mutations that affect growth rates than affect lag times. Genotypic tradeoffs across spontaneous mutations (Box 1, Fig. 2a) are especially important here, because if spontaneous mutations entail a tradeoff across two growth traits, then evolution will be constrained to a narrower range of phenotypes, regardless of selection. Previous studies have measured the supply of variation in growth traits for various combinations of traits and genetic variants, including lag times, growth rates, and yields of *E. coli* [77–80] and *S. cerevisiae* [81] gene deletion strains, a collection of yeast hybrids [68], and a set of *E. coli* strains with point mutations in the adenylate kinase protein [46] (Fig. 2f). In general, these measurements show that mutations are almost always pleiotropic, affecting multiple phases of growth simultaneously, but generally do not show significant tradeoffs; sometimes the are even positive correlations, in which individual mutations tend to improve multiple traits simultaneously. Future work will require more systematic measurements of large mutant libraries in different environments, as well as the development of mechanistic models — for example, based on whole-genome metabolism [82] or intracellular resource allocation [83] — to predict how mutations affect growth traits.

Given a supply of genetic variation in growth traits, the second step of evolution is selection on that variation (Fig. 3f). While laboratory competition experiments can empirically measure this process [84, 85], it is especially amenable to mathematical models of population dynamics, which have, for example, shown how selection acts on variation in lag times vs. growth rates [45, 73, 80], maximum growth rates vs. deceleration rates [53, 86], and secondary growth phases such as fermentation vs. respiration in yeast [76]. In general, we can think of selection as a force vector in the space of growth traits (Fig. 3f). The aforementioned models and experimental data determine the components of this selection force across different traits (allocation of the total selection budget mentioned, Fig. 3c,e). For example, in a well-mixed culture, the yield determines the relative allocation of selection on the lag and growth phases, but there is no component of selection on yield itself [73].

How much of the evolved population dynamics is due to the mutation supply versus selection on the growth traits? Evolution experiments in both *E. coli* [60, 87] and *S. cerevisiae* [88–90] found significant evolutionary change in some growth traits but not others, suggesting that the mutation supply was limited for some of those traits. An important aspect of this question is that patterns of traits may qualitatively differ across lineages within a population (Fig. 2b) compared to lineages in independent populations (Fig. 2c). For example, even if there is no tradeoff across spontaneous mutations for two traits, there can still be a tradeoff across lineages within a single population since the traits of those lineages will cluster along the contour of constant fitness (Fig. 3f) [91], while lineages across independent populations will show a positive correlation due to stochastic variation in the number of fixed mutations (Fig. 3f) [80]. As with the supply of mutations, we still need more data of growth traits within and between evolved populations, ideally over long evolution experiments.

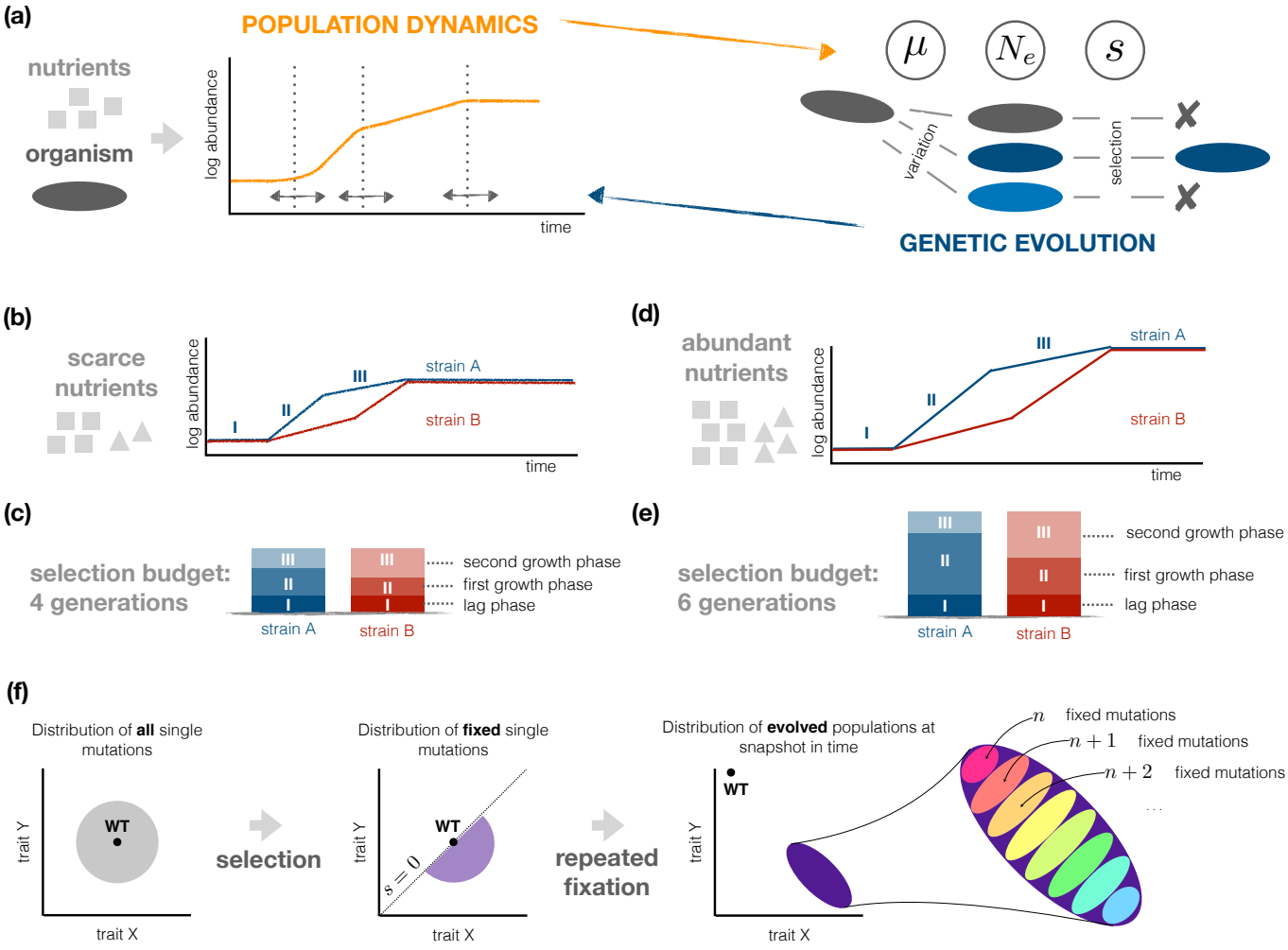

FIG. 3. **Evolution of microbial population dynamics.** (a) Schematic diagram for the influence of population dynamics (orange arrow) on parameters of evolution (black circles) and the resulting evolutionary dynamics (genealogy of blue and grey cells). From an ancestor (dark grey cell), cells with different genotypes appear via mutation (blue cells), but only one of them survives to fixation (dark blue cell) while the others go extinct (grey crosses). The outcome of genetic evolution influences the population dynamics (orange arrow) by changing the organismic growth traits, and thus changing the timing of individual growth phases (dotted lines) in the growth curve (orange curve). The exact growth curve also depends on the input nutrients (grey squares). (b) Schematic growth curves for two species with different patterns of growth phases. Strains A (blue line) and B (red line) both have the same lag phase (marked as I), but strain A grows faster in the first phase of exponential growth (II), whereas strain B grows faster in the second phase of exponential growth (III). (c) Schematic allocation of selection pressure for the two growth curves in panel (b). The height of each bar represents the selection pressure. Both strains have equal total height (4 generations), but different relative allocation of selection pressure to the growth phases (marked by the same roman numerals as in panel (b)). (d) Similar to (b), but with a higher initial amount of nutrients (grey squares and triangles) and greater resulting fold-change. (e) Similar to (c), but for the growth curves in panel (d). The total budget of selection has increased, due to a larger number of initial resources and greater fold-change, compared in panel (c). (f) Diagram for the two step process of evolution on microbial growth traits. First, mutation generates variation in trait space (grey cloud; left panel). Then selection acts to fix mutations with beneficial effects, leading to a distribution of fixed mutations (transparent purple; center-left panel) over replicate populations. Finally, after many repeated rounds of mutation and fixation, the independent replicate populations form a distribution in trait space that is negatively correlated between populations (dark purple cloud; center-right panel) but shows positive correlation within population (oval shapes with different color; right panel).

Ultimately population dynamics and evolution form a feedback loop over time (Fig. 3a) [76]: population dynamics set constraints for evolution over short times, but then evolution changes those constraints over long times. Previous work on the evolution of the half-saturation concentration K in the Monod growth response provides a useful example [53]. At first, the trait K sets the population dynamics by determining the phases of maximum growth and deceleration, which shapes evolution by determining the allocation of selection for mutations to each

of these phases (Fig. 3b–e). But as the trait K evolves to lower concentrations, the population dynamics change: the phase of deceleration becomes shorter and shorter, until the population dynamics are almost entirely at maximum speed. This means there is little selection on additional mutations to K.

IV. OUTLOOK

In recent years we have made great progress toward understanding the population dynamics of microbes in natural environments. This holds the promise of helping us control microbial growth in clinical and environmental systems — for example, promoting the growth of commensal bacteria or inhibiting the growth of a pathogen. However, future progress will hinge on our ability to make these measurements more accurate and systematic; we expect this will require a combination of experimental innovations as well as insights from modeling, especially in terms of identifying better snapshot biomarkers of cellular birth and death. We have also learned a great deal, both theoretically and empirically, about how ecology and evolution may give rise to these observed population dynamics. Here we also look forward to improvements in high-throughput growth phenotyping, especially for large mutant libraries and within-community strain libraries, as well as multiscaling modeling that can predict mutation effects on growth traits. Altogether these steps will help us toward our ultimate goal of a quantitative and predictive theory of microbial population dynamics.

DECLARATION OF INTEREST

None

ACKNOWLEDGMENTS

JWF and MM acknowledge support from an Ambizione grant of the Swiss National Science Foundation (PZ00P3_180147).

[1] Human Microbiome Project Consortium. Structure, function and diversity of the healthy human microbiome. *Nature*, 486:207–14, 2012.

[2] L. R. Thompson, J. G. Sanders, D. McDonald, A. Amir, J. Ladau, K. J. Locey, R. J. Prill, A. Tripathi, S. M. Gibbons, G. Ackermann, J. A. Navas-Molina, S. Janssen, E. Kopylova, Y. Vázquez-Baeza, A. González, J. T. Morton, S. Mirarab, Z. Zech Xu, L. Jiang, M. F. Haroon, J. Kanbar, Q. Zhu, S. Jin Song, T. Kosciolek, N. A. Bokulich, J. Lefler, C. J. Brislawn, G. Humphrey, S. M. Owens, J. Hampton-Marcell, D. Berg-Lyons, V. McKenzie, N. Fierer, J. A. Fuhrman, A. Clauset, R. L. Stevens, A. Shade, K. S. Pollard, K. D. Goodwin, J. K. Jansson, J. A. Gilbert, R. Knight, and The Earth Microbiome Project Consortium. A communal catalogue reveals earth's multiscale microbial diversity. *Nature*, 551:457–463, 2017.

[3] S. Sunagawa, S. G. Acinas, P. Bork, C. Bowler, Tara Oceans Coordinators, D. Eveillard, G. Gorsky, L. Guidi, D. Iudicone, E. Karsenti, F. Lombard, H. Ogata, S. Pesant, M. B. Sullivan, P. Wincker, and C. de Vargas. Tara oceans: towards global ocean ecosystems biology. *Nat Rev Microbiol*, 18:428–445, 2020.

[4] H. Shi, Q. Shi, B. Grodner, J. S. Lenz, W. R. Zipfel, I. L. Brito, and I. De Vlaminck. Highly multiplexed spatial mapping of microbial communities. *Nature*, 588:676–681, 2020.

[5] R. Hatzenpichler, V. Krukenberg, R. L. Spietz, and Z. J. Jay. Next-generation physiology approaches to study microbiome function at single cell level. *Nat Rev Microbiol*, 18:241–256, 2020.

[6] A. M. Martin-Platero, B. Cleary, K. Kauffman, S. P. Preheim, D. J. McGillicuddy, E. J. Alm, and M. F. Polz. High resolution time series reveals cohesive but short-lived communities in coastal plankton. *Nat Commun*, 9:266, 2018.

[7] C. A. Thaiss, D. Zeevi, M. Levy, G. Zilberman-Schapira, J. Suez, A. C. Tengeler, L. Abramson, M. N. Katz, T. Korem, N. Zmora, Y. Kuperman, I. Biton, S. Gilad, A. Harmelin, H. Shapiro, Z. Halpern, E. Segal, and E. Elinav. Transkingdom control of microbiota diurnal oscillations promotes metabolic homeostasis. *Cell*, 159:514–529, 2014.

[8] D. L. Kirchman. Growth rates of microbes in the oceans. *Ann Rev Mar Sci*, 8:285–309, 2016.

[9] C. Rao, K. Z. Coyte, W. Bainter, R. S. Geha, C. R. Martin, and S. Rakoff-Nahoum. Multi-kingdom ecological drivers of microbiota assembly in preterm infants. *Nature*, 591:633–638, 2021.

[10] C. Wang, Y. Yang, Y. Wang, D. Wang, X. Xu, Y. Wang, L. Li, C. Yang, and T. Zhang. Absolute quantification and genome-centric analyses elucidate the dynamics of microbial populations in anaerobic digesters. *Water Research*, 224:119049, 2022.
*** This is a case study of microbial population dynamics in a wastewater reactor, using a combination of metagenomics and spike-in to estimate taxon-specific death rates from scratch.**

[11] J. Monod. The growth of bacterial cultures. *Annu Rev Microbiol*, 3:371–394, 1949.

[12] F. S. Midani, J. Collins, and R. A. Britton. AMiGA: Software for automated analysis of microbial growth assays. *mSystems*, 6:e00508–21, 2021.

[13] C. Cheng and J. C. Thrash. sparse-growth-curve: a computational pipeline for parsing cellular growth curves with low temporal resolution. *Microbiol Resour Announc*, 10:e00296–21, 2021.

[14] J. G. Harrison, W. J. Calder, B. Shuman, and C. A. Buerkle. The quest for absolute abundance: The use of internal standards for DNA-based community ecology.

Mol Ecol Resour, 21:30–43, 2021.
*** This paper provides a thorough discussion of current methods to measure absolute abundance from sequencing data, using the spike-in of cells or DNA sequences.**

[15] F. Song, J. V. Kuehl, A. Chandran, and A. P. Arkin. A simple, cost-effective, and automation-friendly direct PCR approach for bacterial community analysis. *mSystems*, 6:e00224–21, 2021.

[16] L. S. Zaramela, M. Tjuanta, O. Moyne, M. Neal, and K. Zengler. synDNA—a synthetic dna spike-in method for absolute quantification of shotgun metagenomic sequencing. *mSystems*, 7:e00447–22, 2022.

[17] S. Reitmeier, S. Kiessling, T. Clavel, M. List, E. L. Almeida, T. S. Ghosh, K. Neuhaus, H. Grallert, J. Linseisen, T. Skurk, B. Brandl, T. A. Breuninger, M. Troll, W. Rathmann, B. Linkohr, H. Hauner, M. Laudes, A. Franke, C. I. Le Roy, J. T. Bell, T. Spector, J. Baumbach, P. W. O'Toole, A. Peters, and D. Haller. Arrhythmic gut microbiome signatures predict risk of type 2 diabetes. *Cell Host Microbe*, 28:258–272.e6, 2020.

[18] B. Charlesworth. *Evolution in Age-Structured Populations*. Cambridge University Press, 1994.

[19] J. Jonasson, T. Harkonen, L. Sundqvist, S. V. Edwards, and K. C. Harding. A unifying framework for estimating generation time in age-structured populations: Implications for phylogenetics and conservation biology. *The American Naturalist*, 200:48–62, 2022.
*** This gives a mathematical overview of growth rate estimators used in age-structured populations and a potential inspiration for developing snapshot methods beyond the peak-to-trough ratio.**

[20] T. Korem, D. Zeevi, J. Suez, A. Weinberger, T. Avnit-Sagi, M. Pompan-Lotan, E. Matot, G. Jona, A. Harmelin, N. Cohen, A. Sirota-Madi, C. A. Thaiss, M. Pevsner-Fischer, R. Sorek, R. J. Xavier, E. Elinav, and E. Segal. Growth dynamics of gut microbiota in health and disease inferred from single metagenomic samples. *Science*, 349:1101–1106, 2015.
**** This paper was the first implementation of the peak-to-trough ratio of genome read coverage as a growth rate proxy, with successful validation of the method for *E. coli* in chemostat and batch cultures.**

[21] H. Bremer and G. Churchward. An examination of the Cooper-Helmstetter theory of DNA replication in bacteria and its underlying assumptions. *J Theor Biol*, 69:645–654, 1977.

[22] C. T. Brown, M. R. Olm, R. C. Thomas, and J. F. Banfield. Measurement of bacterial replication rates in microbial communities. *Nat Biotechnol*, 34:1256–1263, 2016.

[23] A. Emiola and J. Oh. High throughput in situ metagenomic measurement of bacterial replication at ultra-low sequencing coverage. *Nat Commun*, 9:4956, 2018.

[24] Y. Gao and H. Li. Quantifying and comparing bacterial growth dynamics in multiple metagenomic samples. *Nat Methods*, 15:1041–1044, 2018.

[25] T. A. Joseph, P. Chlenski, A. Litman, T. Korem, and I. Pe'er. Accurate and robust inference of microbial growth dynamics from metagenomic sequencing reveals personalized growth rates. *Genome Res*, 32:558–568, 2022.

[26] Julia Carroll, Nicolas Van Oostende, and Bess B. Ward. Evaluation of genomic sequence-based growth rate methods for synchronized synechococcus cultures. *Applied and Environmental Microbiology*, 88:e01743–21, 2022.

[27] A. M. Long, S. Hou, J. C. Ignacio-Espinoza, and J. A. Fuhrman. Benchmarking microbial growth rate predictions from metagenomes. *ISME J*, 15:183–195, 2021.
**** The authors assemble a naturalistic dataset of growth rates, measured through absolute abundance in controlled incubation of seawater, across 101 marine taxa. This provides a hard test for the peak-to-trough ratio of genome read coverage as a predictor for population growth rate.**

[28] T. P. Wytock and A. E. Motter. Predicting growth rate from gene expression. *Proc Natl Acad Sci USA*, 116:367–372, 2019.

[29] M. Mori, Z. Zhang, A. Banaei-Esfahani, J.-B. Lalanne, H. Okano, B. C. Collins, A. Schmidt, O. T. Schubert, D.-S. Lee, G.-W. Li, R. Aebersold, T. Hwa, and C. Ludwig. From coarse to fine: The absolute Escherichia coli proteome under diverse growth conditions. *Mol Syst Biol*, 17:e9536, 2021.

[30] C. Culley, S. Vijayakumar, G. Zampieri, and C. Angione. A mechanism-aware and multiomic machine-learning pipeline characterizes yeast cell growth. *Proceedings of the National Academy of Sciences*, 117:18869–18879, 2020.

[31] G. Magazzù, G. Zampieri, and C. Angione. Multimodal regularized linear models with flux balance analysis for mechanistic integration of omics data. *Bioinformatics*, 37:3546–3552, 2021.

[32] N. Arandia-Gorostidi, A. E. Parada, and A. E. Dekas. Single-cell view of deep-sea microbial activity and intra-community heterogeneity. *ISME J*, 17:59–69, 2023.
*** This paper describes growth rate in marine microbial communities across a range of depths, as approximated by incorporation of isotope-labeled nitrogen sources (using nanoSIMS).**

[33] B. J. Koch, T. A. McHugh, M. Hayer, E. Schwartz, S. J. Blazewicz, P. Dijkstra, N. van Gestel, J. C. Marks, R. L. Mau, E. M. Morrissey, J. Pett-Ridge, and B. A. Hungate. Estimating taxon-specific population dynamics in diverse microbial communities. *Ecosphere*, 9:e02090, 2018.
**** This study is an exemplary application of stable-isotope probing (qSIP) to track 300 taxa in their birth, death, and net growth, by incubating a soil sample with heavy water.**

[34] B. Gibson, D. J. Wilson, E. Feil, and A. Eyre-Walker. The distribution of bacterial doubling times in the wild. *Proc R Soc B*, 285:20180789, 2018.
**** The authors devise a clever approach for inferring historical average growth rates of species by comparing their mutation rates measured in different units (generation versus clock time).**

[35] S. Vieira-Silva and E. P. C. Rocha. The systemic imprint of growth and its uses in ecological (meta)genomics. *PLoS Genet*, 6:e1000808, 2010.

[36] J. S. Madin, D. A. Nielsen, M. Brbic, R. Corkrey, D. Danko, K. Edwards, M. K. M. Engqvist, N. Fierer, J. L. Geoghegan, M. Gillings, N. C. Kyrpides, E. Litchman, C. E. Mason, L. Moore, S. L. Nielsen, I. T. Paulsen, N. D. Price, T. B. K. Reddy, M. A. Richards, E. P. C. Rocha, T. M. Schmidt, H. Shaaban, M. Shukla, F. Supek, S. G. Tetu, S. Vieira-Silva, A. R. Wattam, D. A.

Westfall, and M. Westoby. A synthesis of bacterial and archaeal phenotypic trait data. *Sci Data*, 7:170, 2020.

[37] J. L. Weissman, S. Hou, and J. A. Fuhrman. Estimating maximal microbial growth rates from cultures, metagenomes, and single cells via codon usage patterns. *Proc Natl Acad Sci USA*, 118:e2016810118, 2021.
*** This paper provides a comprehensive study of genomic codon usage bias as a predictor of maximum birth rates in an enormous collection of microbial species.**

[38] B. R. K. Roller, S. F. Stoddard, and T. M. Schmidt. Exploiting rRNA operon copy number to investigate bacterial reproductive strategies. *Nat Microbiol*, 1:1–7, 2016.

[39] J. Li, R. L. Mau, P. Dijkstra, B. J. Koch, E. Schwartz, X.-J. A. Liu, E. M. Morrissey, S. J. Blazewicz, J. Pett-Ridge, B. W. Stone, M. Hayer, and B. A. Hungate. Predictive genomic traits for bacterial growth in culture versus actual growth in soil. *ISME J*, 13:2162–2172, 2019.
*** The authors tested rRNA copy number as a predictor for growth rate, using both literature values as well as benchmarking measurements from isotope-labeled soil communities.**

[40] A. D. Letten and W. B. Ludington. Pulsed, continuous or somewhere in between? resource dynamics matter in the optimisation of microbial communities. *ISME J*, 2023.
*** The authors provide an explicit proof-of-principle model showing the importance of population and resource dynamics in modulating community composition.**

[41] A. T. Reese, F. C. Pereira, A. Schintlmeister, D. Berry, M. Wagner, L. P. Hale, A. Wu, S. Jiang, H. K. Durand, X. Zhou, R. T. Premont, A. M. Diehl, T. M. O'Connell, S. C. Alberts, T. R. Kartzinel, R. M. Pringle, R. R. Dunn, J. P. Wright, and L. A. David. Microbial nitrogen limitation in the mammalian large intestine. *Nat Microbiol*, 3:1441–1450, 2018.

[42] M. A. Saito, T. J. Goepfert, and J. T. Ritt. Some thoughts on the concept of colimitation: Three definitions and the importance of bioavailability. *Limnol Oceanogr*, 53:276–290, 2008.

[43] F. Dini-Andreote, M. de Cássia Pereira e Silva, X. Triadó-Margarit, E. O. Casamayor, J. D. van Elsas, and J. F. Salles. Dynamics of bacterial community succession in a salt marsh chronosequence: Evidences for temporal niche partitioning. *ISME J*, 8:1989–2001, 2014.

[44] P. Chesson. Multispecies competition in variable environments. *Theor Popul Biol*, 45:227–276, 1994.

[45] M. Manhart and E. I. Shakhnovich. Growth tradeoffs produce complex microbial communities on a single limiting resource. *Nat Commun*, 9:3214, 2018.

[46] B. V. Adkar, M. Manhart, S. Bhattacharyya, J. Tian, M. Musharbash, and E. I. Shakhnovich. Optimization of lag phase shapes the evolution of a bacterial enzyme. *Nat Ecol Evol*, 1:0149, 2017.

[47] M. Basan, T. Honda, D. Christodoulou, M. Hörl, Y.-F. Chang, E. Leoncini, A. Mukherjee, H. Okano, B. R. Taylor, J. M. Silverman, C. Sanchez, J. R. Williamson, J. Paulsson, T. Hwa, and U. Sauer. A universal tradeoff between growth and lag in fluctuating environments. *Nature*, 584:470–474, 2020.

[48] T. Pfeiffer and S. Bonhoeffer. Evolution of cross-feeding in microbial populations. *Am Nat*, 163:E126–E135, 2004.

[49] I. Gudelj, J. S. Weitz, T. Ferenci, M. C. Horner-Devine, C. J. Marx, J. R. Meyer, and S. E. Forde. An integrative approach to understanding microbial diversity: From intracellular mechanisms to community structure. *Ecol Lett*, 13:1073–1084, 2010.

[50] J. R. Meyer, I. Gudelj, and R. Beardmore. Biophysical mechanisms that maintain biodiversity through trade-offs. *Nat Commun*, 6:6278, 2015.

[51] D. Tilman and S. S. Kilham. Phosphate and silicate growth and uptake kinetics of the diatoms Asterionella formosa and Cyclola meneghiniana in batch and semi-continuous culture. *J Phycol*, 12:375–383, 1976.

[52] N. Ziv, M. L. Siegal, and D. Gresham. Genetic and nongenetic determinants of cell growth variation assessed by high-throughput microscopy. *Mol Biol Evol*, 30:2568–2578, 2013.

[53] J. W. Fink, N. A. Held, and M. Manhart. Microbial population dynamics decouple growth response from environmental nutrient concentration. *Proc Natl Acad Sci USA*, 120:e2207295120, 2023.
*** This paper assembles a comprehensive collection of measurements for microbial growth rate dependence on nutrient concentrations, and uses a mathematical model to demonstrate how different regimes of population dynamics lead to qualitatively-different evolutionary outcomes for this dependence.**

[54] R. C. MacLean. The tragedy of the commons in microbial populations: insights from theoretical, comparative and experimental studies. *Heredity*, 100:471–477, 2007.

[55] J.-N. Jasmin and C. Zeyl. Life-history evolution and density-dependent growth in experimental populations of yeast. *Evolution*, 66:3789–3802, 2012.

[56] J.-N. Jasmin, M. M. Dillon, and C. Zeyl. The yield of experimental yeast populations declines during selection. *Proc R Soc B*, 279:4382–4388, 2012.

[57] H. Bachmann, M. Fischlechner, I. Rabbers, N. Barfa, F. B. dos Santos, D. Molenaar, and B. Teusink. Availability of public goods shapes the evolution of competing metabolic strategies. *Proc Natl Acad Sci USA*, 110:14302–14307, 2013.

[58] L. S. Luckinbill. r and K selection in experimental populations of Escherichia coli. *Science*, 202:1201–1203, 1978.

[59] G. J. Velicer and R. E. Lenski. Evolutionary trade-offs under conditions of resource abundance and scarcity: Experiments with bacteria. *Ecology*, 80:1168–1179, 1999.

[60] M. Novak, T. Pfeiffer, R. E. Lenski, U. Sauer, and S. Bonhoeffer. Experimental tests for an evolutionary trade-off between growth rate and yield in E. coli. *Am Nat*, 168:242–251, 2006.

[61] J. M. Fitzsimmons, S. E. Schoustra, J. T. Kerr, and R. Kassen. Population consequences of mutational events: effects of antibiotic resistance on the r/K trade-off. *Evol Ecol*, 24:227–236, 2010.

[62] J. Warringer, E. Zörgö, F. A. Cubillos, A. Zia, A. Gjuvsland, J. T. Simpson, A. Forsmark, R. Durbin, S. W. Omholt, E. J. Louis, G. Liti, A. Moses, and A. Blomberg. Trait variation in yeast is defined by population history. *PLOS Genet*, 7:e1002111, 2011.

[63] C. Reding-Roman, M. Hewlett, S. Duxbury, F. Gori, I. Gudelj, and R. Beardmore. The unconstrained evolution of fast and efficient antibiotic-resistant bacterial genomes. *Nat Ecol Evol*, 1:0050, 2017.

[64] C. Cheng, E. J. O'Brien, D. McCloskey, J. Utrilla, C. Olson, R. A. LaCroix, T. E. Sandberg, A. M. Feist, B. O. Palsson, and Z. A. King. Laboratory evolution re-

veals a two-dimensional rate-yield tradeoff in microbial metabolism. *PLoS Comput Biol*, 15:e1007066, 2019.

[65] I. A. M. Swinnen, K. Bernaerts, E. J. J. Dens, A. H. Geeraerd, and J. F. Van Impe. Predictive modelling of the microbial lag phase: a review. *Int J Food Microbiol*, 94:137–159, 2004.

[66] Y. Himeoka and K. Kaneko. Theory for transitions between exponential and stationary phases: Universal laws for lag time. *Phys Rev X*, 7:021049, 2017.

[67] J. Wang, E. Atolia, B. Hua, Y. Savir, R. Escalante-Chong, and M. Springer. Natural variation in preparation for nutrient depletion reveals a cost-benefit tradeoff. *PLOS Biol*, 13:e1002041, 2015.

[68] N. Ziv, B. M. Shuster, M. L. Siegal, and D. Gresham. Resolving the complex genetic basis of phenotypic variation and variability of cellular growth. *Genetics*, 206:1645–1657, 2017.

[69] R. E. Beardmore, I. Gudelj, D. A. Lipson, and L. D. Hurst. Metabolic trade-offs and the maintenance of the fittest and the flattest. *Nature*, 472:342–346, 2011.

[70] K. W. Wirtz. A generic model for changes in microbial kinetic coefficients. *J Biotechnol*, 97:147–162, 2002.

[71] E. Litchman, C. A. Klausmeier, O. M. Schofield, and P. G. Falkowski. The role of functional traits and trade-offs in structuring phytoplankton communities: scaling from cellular to ecosystem level. *Ecol Lett*, 10:1170–1181, 2007.

[72] M. T. Wortel. Evolutionary coexistence in a fluctuating environment by specialization on resource level. *bioRxiv*, 2022. doi:10.1101/2021.05.18.444718.

[73] M. Manhart, B. V. Adkar, and E. I. Shakhnovich. Trade-offs between microbial growth phases lead to frequency-dependent and non-transitive selection. *Proc R Soc B*, 285:20172459, 2018.

[74] B. Bloxham, H. Lee, and J. Gore. Diauxic lags explain unexpected coexistence in multi-resource environments. *Mol Syst Biol*, 18:e10630, 2022.
**** This paper provides the most explicit demonstration of a growth rate tradeoff in a coexisting community of species.**

[75] W. J. Ewens. *Mathematical Population Genetics*. Springer-Verlag, New York, 2004.

[76] D. Collot, T. Nidelet, J. Ramsayer, O. C. Martin, S. Méléard, C. Dillmann, D. Sicard, and J. Legrand. Feedback between environment and traits under selection in a seasonal environment: consequences for experimental evolution. *Proc R Soc B*, 285:20180284, 2018.

[77] R. Takeuchi, T. Tamura, T. Nakayashiki, Y. Tanaka, A. Muto, B. L. Wanner, and H. Mori. Colony-live — a high-throughput method for measuring microbial colony growth kinetics — reveals diverse growth effects of gene knockouts in Escherichia coli. *BMC Microbiol*, 14:171, 2014.

[78] G. Chevereau, M. Dravecká, T. Batur, A. Guvenek, D. H. Ayhan, E. Toprak, and T. Bollenbach. Quantifying the determinants of evolutionary dynamics leading to drug resistance. *PLOS Biol*, 13:e1002299, 2015.

[79] M. Campos, S. K. Govers, I. Irnov, G. S. Dobihal, F. Cornet, and C. Jacobs-Wagner. Genomewide phenotypic analysis of growth, cell morphogenesis, and cell cycle events in Escherichia coli. *Mol Syst Biol*, 14:e7573, 2018.

[80] J. Lin, M. Manhart, and A. Amir. Evolution of microbial growth traits under serial dilution. *Genetics*, 215:767–777, 2020.

[81] J. Warringer, E. Ericson, L. Fernandez, O. Nerman, and A. Blomberg. High-resolution yeast phenomics resolves different physiological features in the saline response. *Proc Natl Acad Sci USA*, 100:15724–15729, 2003.

[82] J. M. Monk, C. J. Lloyd, E. Brunk, N. Mih, A. Sastry, Z. King, R. Takeuchi, W. Nomura, Z. Zhang, H. Mori, A. M. Feist, and B. O. Palsson. I ML1515, a knowledgebase that computes Escherichia coli traits. *Nat Biotechnol*, 35:904–908, 2017.

[83] S. Sharma and R. Steuer. Modelling microbial communities using biochemical resource allocation analysis. *J R Soc Interface*, 16:20190474, 2019.

[84] Y. Li, S. Venkataram, A. Agarwala, B. Dunn, D. A. Petrov, G. Sherlock, and D. S. Fisher. Hidden complexity of yeast adaptation under simple evolutionary conditions. *Curr Biol*, 28:515–525, 2018.

[85] Y. Li, D. A. Petrov, and G. Sherlock. Single nucleotide mapping of trait space reveals Pareto fronts that constrain adaptation. *Nat Ecol Evol*, 3:1539–1551, 2019.

[86] F. M. Stewart and B. R. Levin. Partitioning of resources and the outcome of interspecific competition: A model and some general considerations. *Am Nat*, 107:171–198, 1973.

[87] F. Vasi, M. Travisano, and R. E. Lenski. Long-term experimental evolution in Escherichia coli. II. Changes in life-history traits during adaptation to a seasonal environment. *Am Nat*, 144:432–456, 1994.

[88] D. Dykhuizen and D. Hartl. Evolution of competitive ability in Escherichia coli. *Evolution*, 35:581, 1981.

[89] Karin Kovárŏvá. *Growth Kinetics of Escherichia Coli: Effect of Temperature, Mixed Substrate Utilization and Adaptation to Carbon-Limited Growth*. PhD thesis, ETH Zurich, Zurich, Switzerland, 1996.

[90] J. Adams, C. Paquin, P. W. Oeller, and L. W. Lee. Physiological characterization of adaptive clones in evolving populations of the yeast, Saccharomyces cerevisiae. *Genetics*, 110:173–185, 1985.

[91] K. Gomez, J. Bertram, and J. Masel. Directional selection rather than functional constraints can shape the G matrix in rapidly adapting asexuals. *Genetics*, 211:715–729, 2019.